Thermal and magnetic properties of spin-1 magnetic chain compounds with large single-ion and in-plane anisotropies

M. T. Batchelor, Xi-Wen Guan, and Norman Oelkers

Department of Theoretical Physics, Research School of Physical Sciences and Engineering and Mathematical Sciences Institute,
Australian National University, Canberra ACT 0200, Australia

The thermal and magnetic properties of spin-1 magnetic chain compounds with large single-ion and in-plane anisotropies are investigated via the integrable $su(3)$ model in terms of the quantum transfer matrix method and the recently developed high temperature expansion method for exactly solved models. It is shown that large single-ion anisotropy may result in a singlet gapped phase in the spin-1 chain which is significantly different from the standard Haldane phase. A large in-plane anisotropy may destroy the gapped phase. On the other hand, in the vicinity of the critical point a weak in-plane anisotropy leads to a different phase transition than the Pokrovsky-Talapov transition. The magnetic susceptibility, specific heat, and magnetization evaluated from the free energy are in excellent agreement with the experimental data for the compounds $Ni(C_2H_8N_2)_2Ni(CN)_4$ and $Ni(C_{10}H_8N_2)_2Ni(CN)_4 \cdot H_2O$.

I. INTRODUCTION

Haldane's[1] conjecture that spin-S chains exhibit an energy gap in the lowest magnon excitation for $2S$ even with no significant gap for $2S$ odd inspired a great deal of experimental and theoretical investigation. Rich and novel quantum magnetic effects, including valence-bond-solid Haldane phases and dimerized phases,[2,3] fractional magnetization plateaux[4] and spin-Peierls transitions[5] have since been found in low-dimensional spin systems. In this light, the spin-1 Heisenberg magnets have been extensively studied in Haldane gapped materials.[6,7] The valence-bond-solid ground state and the dimerized state form the Haldane phase with an energy gap.[2] The Haldane gap in integer spin chains may close in the presence of additional biquadratic terms or in-plane anisotropies. In particular a large single-ion anisotropy may result in a singlet ground state[8,9] which is significantly different from the standard Haldane phase.

The difference between the two gapped phases appears to arise from the ground state and excitations. In the Haldane nondegenerate ground state, a single valence bond connects each neighbouring pair to form a singlet. An expected excitation comes from breaking down the valence bond solid state where a nonmagnetic state $S_i=0$ at site i is substituted for a state $S_i=1$. In this way a total spin $S=1$ excitation causes an energy gap referred to as the Haldane gap. Whereas the large-anisotropy-induced gapped phase in the spin-1 chain is caused by trivalent orbital splitting. For a large single-ion anisotropy, the singlet can occupy all states such that the ground state lies in the nondegenerate gapped phase. The lowest excitation arises as the lower component of the doublet is involved in the ground state. This excitation results in the energy gap.

A number of spin-1 magnetic chain compounds have been identified as planar Heisenberg magnetic chains with large anisotropy. These include $Ni(C_2H_8N_2)_2Ni(CN)_4$ (abbreviated NENC), $Ni(C_{11}H_{10}N_2O)_2Ni(CN)_4$ (abbreviated NDPK),[10,11] and $Ni(C_{10}H_8N_2)_2Ni(CN)_4 \cdot H_2O$ (abbreviated NBYC).[12]

This kind of system exhibits a nondegenerate ground state which can be separated from the lowest excitation. This gapped phase also occurs in some nickel salts with a large zero-field splitting, such as $NiSnCl_6 \cdot 6H_2O$,[13] $[Ni(C_5H_5NO)_6](ClO_4)_2$,[14] and $Ni(NO_3)_2 \cdot 6H_2O$.[15] The theoretical study of these compounds relies on a molecular field approximation for the Van Vleck equation.[16] To first-order Van Vleck approximation, the exchange interaction is neglected. To obtain a good fit to the experimental data an effective crystalline field has to be incorporated. This approximation causes uncertainties and discrepancies in fitting the experimental data. Here we take a new approach via the theory of integrable models.

It has been recently demonstrated[17] that integrable models can be used to study real ladder compounds via the thermodynamic Bethe ansatz[18] (TBA) and the exact high temperature expansion (HTE) method.[19,20] In this paper we present an integrable spin-1 chain with additional terms to account for planar single-ion anisotropy and in-plane anisotropy. The ground state properties and the thermodynamics of the chains are studied via the TBA and HTE. We show that a large planar single-ion anisotropy results in a nondegenerate singlet ground state which is significantly different from the Haldane phases found in Haldane gapped materials.[6,7] We examine the thermal and magnetic properties of the compounds NENC[10,11] and NBYC.[12] Excellent agreement between our theoretical results and the experimental data for the magnetic susceptibility, specific heat and magnetization confirms that the strong single-ion anisotropy, which is induced by an orbital splitting, can dominate the low temperature behavior of this class of compounds. Our exact results for the integrable spin-1 model may provide widespread application in the study of thermal and magnetic properties of other real compounds, such as NDPK[10,11] and certain nickel salts.[13–16]

II. THE INTEGRABLE SPIN-1 MODEL

In contrast to the standard Heisenberg spin-1 materials, experimental measurements on the new spin-1 compound

$LiVGe_2O_6$[21] and the compounds NENC and NBYC[10,12] exhibit unexpected behavior, possibly due to the presence of biquadratic interaction and a strong single-ion anisotropy, making it very amenable to our approach. The axial distortion of the crystalline field in the compounds NENC and NBYC results from the triplet $^3A_{2g}$ splitting. Specifically, the triplet orbit splits into a low-lying doublet (d_{xy}, d_{yz}) and a singlet orbital (d_{xz}) at an energy Δ_{CF} above the doublet. Inspired by the high temperature magnetic properties of this kind of material, we consider an integrable spin-1 chain with Hamiltonian

$$\mathcal{H} = J\mathcal{H}_0 + D\sum_{j=1}^{N}(S_j^z)^2 + E\sum_{j=1}^{N}[(S_j^x)^2 - (S_j^y)^2] - \mu_B gH\sum_{j=1}^{N}S_j^z, \tag{1}$$

$$\mathcal{H}_0 = \sum_{j=1}^{N}\{\vec{S}_j \cdot \vec{S}_{j+1} + (\vec{S}_j \cdot \vec{S}_{j+1})^2\}.$$

$\mathcal{H}_0$ is the standard $su(3)$ integrable spin chain, which is well understood.[22–25] Here $\vec{S}_i$ denotes the spin-1 operator at site i, N is the number of sites and periodic boundary conditions apply. The constants J, D and E denote exchange spin-spin coupling, single-ion anisotropy and in-plane anisotropy, respectively. The Bohr magneton is denoted by μ_B and g is the Landé factor. We consider only antiferromagnetic coupling, i.e., $J > 0$ and $D > 0$.

A. The ground state at zero temperature

For the sake of simplicity in analyzing the ground state properties at zero temperature, we first take $E = 0$, i.e., no in-plane anisotropy. In this case Hamiltonian (1), which can be derived from the $su(3)$ row-to-row quantum transfer matrix with appropriate chemical potentials in the fundamental basis, is integrable by the Bethe ansatz. The energy is given by

$$\mathcal{E} = -J\sum_{j=1}^{M_1}\frac{1}{(v_j^{(1)})^2 + \frac{1}{4}} - DN_0 - \mu_B gH(N_+ - N_-), \tag{2}$$

where the parameters $v_j^{(1)}$ satisfy the Bethe equations[22,23]

$$\prod_{i=1}^{M_{k-1}}\frac{v_j^{(k)} - v_i^{(k-1)} + i/2}{v_j^{(k)} - v_i^{(k-1)} - i/2} = \prod_{\substack{l=1 \\ l \neq j}}^{M_k}\frac{v_j^{(k)} - v_l^{(k)} + i}{v_j^{(k)} - v_l^{(k)} - i}$$

$$\times \prod_{l=1}^{M_{k+1}}\frac{v_j^{(k)} - v_l^{(k+1)} - i/2}{v_j^{(k)} - v_l^{(k+1)} + i/2}. \tag{3}$$

In the above, $k = 1, 2$ and $j = 1, \ldots, M_k$ and the conventions $v_j^{(0)} = v_j^{(3)} = 0$, $M_3 = 0$ apply. N_+, N_0, N_- denote the number of sites with spin $S^z = 1$, 0, -1 in the Bethe eigenstates. In the thermodynamic limit, the Bethe ansatz equations (3) admit complex string solutions[18] from which the TBA equations can be derived.[26,27] Following the standard TBA analysis, we find that the ground state in the zero temperature limit is
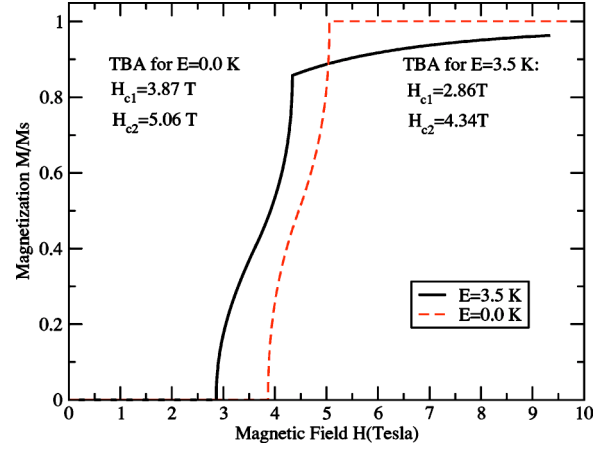

FIG. 1. (Color online) Magnetization versus magnetic field H in units of saturation magnetization for Hamiltonian (1) with $J = 0.2$ K, $D = 6$ K, $E = 3.5$, and 0 K, $g = 2.0$ with parallel magnetic field. The solid and dashed lines denote the magnetization derived from the TBA with $E = 3.5$ K and $E = 0$ K, respectively. The magnetization curve for $E = 3.5$ K indicates different quantum phase transitions in the vicinity of H_{c1} and H_{c2} than for the $E = 0$ K square root field-dependent critical behavior in the absence of the in-plane anisotropy.

gapped if the single-ion anisotropy $D > 4J$. The singlet ground state is separated from the lowest spin excitation by an energy gap $\Delta = D - 4J$. This energy gap is decreased by the external magnetic field H. At the critical point $H_{c1} = (D - 4J)/\mu_B g$, the singlet ground state breaks down. Due to the magnon excitation, the magnetization almost linearly increases with the magnetic field. Once the magnetic field is increased beyond the second critical point $H_{c2} = (D + 4J)/\mu_B g$ the ground state is fully polarized, i.e., in the $M = M_s$ plateau region. The magnetization derived from the TBA is shown in Fig. 1. We remark that a gapped phase exists only for anisotropy values satisfying the "strong anisotropy" condition $D > 4J$. As shown in Refs. 26 and 27 for the spin ladders, the magnetization in the vicinity of the critical fields H_{c1} and H_{c2} depends on the square root of the field, indicating a Pokrovsky-Talapov transition. In this regime, the anisotropy effects overwhelm the contribution from the biquadratic interaction and open a gapped phase in the ground state.

When $E \neq 0$, the in-plane anisotropy $x^2 - y^2$ breaks the z^2 symmetry and weakens the energy gap. In the presence of the in-plane anisotropy term E, the energies split into three levels with respect to the new basis $\phi_0 = |0\rangle$ and $\phi_\pm = a_\pm|-1\rangle + |1\rangle$, with $a_\pm = [\mu_B gH \pm \sqrt{(\mu_B gH)^2 + E^2}]/E$. In this basis the eigenvalues of the underlying permutation operator are the same as the eigenvalues using the fundamental basis. The model thus remains integrable. We find that if $E < D$, there is still a gapped phase with gap $\Delta = D - 4J - \sqrt{(\mu_B gH)^2 + E^2}$ for the region $H < H_{c1}$. Here the critical field $H_{c1} = \sqrt{(D - 4J)^2 - E^2}/\mu_B g$. In this gapped phase the ground state is the non-degenerate singlet. Subsequently, when $H > H_{c1}$ the state ϕ_- gets involved in the ground state. At the critical point H_{c1}, the phase transition is not of the Pokrovsky-Talapov type due to the mixture of a doublet state

in the ϕ_- state. The magnetization increases as the magnetic field increases. Past the second critical point $H_{c2} = \sqrt{(D+4J)^2 - E^2}/\mu_B g$, the singlet state is no longer involved in the ground state. The state ϕ_- fully occupies the ground state. As the magnetic field is increased beyond H_{c2}, the (normalized) magnetization $M = H/\sqrt{H^2 + (E/\mu_B g)^2}$ gradually approaches $M_s = 1$. These novel phase transition may be observed from the low temperature magnetization curve, which can be evaluated from the TBA equations at $T = 0$, as per the example in Fig. 1. It shows that the gap sensitively depends on the single-ion anisotropy and the in-plane anisotropy. These phase transitions disappear at high temperatures. In addition, the inflection point at $H = \sqrt{D^2 - E^2}/\mu_B g$ and $M = 1/2 \sqrt{1 - (E/D)^2}$ indicates that the probabilities of the components ϕ_0 and ϕ_- are equal. Moreover, if the exchange interaction decreases, the magnetization in the vicinity of the critical point H_{c1} increases steeply. For $J = 0$, i.e., the case of independent spins, the critical points H_{c1} and H_{c2} merge into one point, at which a discontinuity in the magnetization occurs. For $D < 4J + E$, there is no gapped phase.

B. Magnetic properties at high temperature

In order to study thermodynamic properties, we adopt the quantum-transfer-matrix (QTM) approach.[28] Explicitly, following[20] the eigenvalue of the QTM for the model (1) (up to a constant) is given by

$$
T_1^{(1)}(v, \{v_i^{(a)}\}) = e^{\beta\mu_1}\phi_-(v-i)\phi_+(v)\frac{Q_1(v+i/2)}{Q_1(v-i/2)}
$$
$$
+ e^{\beta\mu_2}\phi_-(v)\phi_+(v)\frac{Q_1(v-3i/2)Q_2(v)}{Q_1(v-i/2)Q_2(v-i)}
$$
$$
+ e^{\beta\mu_3}\phi_-(v)\phi_+(v+i)\frac{Q_2(v-2i)}{Q_2(v-i)}. \quad (4)
$$

In the above equation the chemical potential terms are

$$
\mu_1 = \mu_B g H, \quad \mu_2 = D, \quad \mu_3 = -\mu_B g H, \quad (5)
$$

where for the moment we take $E = 0$. We have adopted the notation from Ref. 20 with $\phi_\pm(v) = (v \pm i u_N)^{N/2}$, $Q_a(v) = \prod_{i=1}^{M_a}(v - v_i^{(a)})$ for $a = 1, 2$, and $Q_0(v) = 1$. Here $u_N = -J\beta/N$ where N is the Trotter number. Following the HTE scheme,[20] we derive the high temperature expansion for the free energy of model (1) in powers of J/T. Because the expansion parameter J/T is small for weak intrachain coupling J, we may expect the free energy to accurately describe the thermodynamic quantities at sufficiently high temperatures, even for a small number of terms. To third order, the result is

$$
-\frac{1}{T}f(T,H) = \ln C_0 + C_{1,0}^1 \frac{J}{T} + C_{2,0}^1 \left(\frac{J}{T}\right)^2 + C_{3,0}^1 \left(\frac{J}{T}\right)^3 + \cdots.
$$
$$(6)$$

The coefficients $C_{b,0}^1$, $b = 1, 2, 3$, are given by[20]

$$
C_{1,0}^1 = 2A_+,
$$

$$
C_{2,0}^1 = 3A_+(1 - 2A_+) + 3A_-,
$$

$$
C_{3,0}^1 = \frac{10}{3}A_+\left(1 - \frac{27}{5}A_+ + 8A_+^2\right) + 8A_-(1 - 3A_+), \quad (7)
$$

with

$$
C_0 = B_{0,D},
$$

$$
A_+ = B_{D,0}/B_{0,D}^2,
$$

$$
A_- = \exp(D/T)/B_{0,D}^3,
$$

$$
B_{x,y} = 2\exp(x/T)\cosh(\mu_B g H/T) + \exp(y/T). \quad (8)
$$

For later use, we also give the HTE free energy with in-plane rhombic anisotropy E. If the external magnetic field is parallel to the z axis, the chemical potentials in Eq. (4) become

$$
\mu_1 = h, \quad \mu_2 = D, \quad \mu_3 = -h, \quad (9)
$$

where $h = \sqrt{E^2 + (\mu_B g_\parallel H)^2}$. In this case the function $B_{x,y}$ in Eq. (8) changes to

$$
B_{x,y} = 2\exp(x/T)\cosh(h/T) + \exp(y/T). \quad (10)
$$

On the other hand, if we apply a perpendicular magnetic field to the Hamiltonian (1), the chemical potential terms in Eq. (4) are replaced by

$$
\mu_1 = \frac{1}{2}(D - E + h'),
$$

$$
\mu_2 = E,
$$

$$
\mu_3 = \frac{1}{2}(D - E - h'), \quad (11)
$$

where $h' = \sqrt{(D+E)^2 + 4g_\perp^2 \mu_B^2 H_a^2}$ with $a = x$ or y.[29] Subsequently, we have

$$
C_0 = B_{(D-E)/2,D},
$$

$$
A_+ = B_{(D+E)/2,D-E}/B_{(D-E)/2,D}^2,
$$

$$
A_- = \exp(D/T)/B_{(D-E)/2,D}^3, \quad (12)
$$

with now $B_{x,y} = 2\exp(x/T)\cosh(h'/T) + \exp(y/T)$.

Equation (6) for the free energy $f(T,H)$ is our key result. Physical properties such as the susceptibility, magnetization and the specific heat follow in the usual way by differentiation. We also use $f(T,H)$ to calculate the phase diagram for both $T \simeq 0$ K and finite temperatures (see Fig. 6). We find that considering up to 3rd order in J/T is sufficient as higher orders are negligibly small. This is in stark contrast to other series expansions which need many orders to accurately describe physical properties. This is mainly because here the
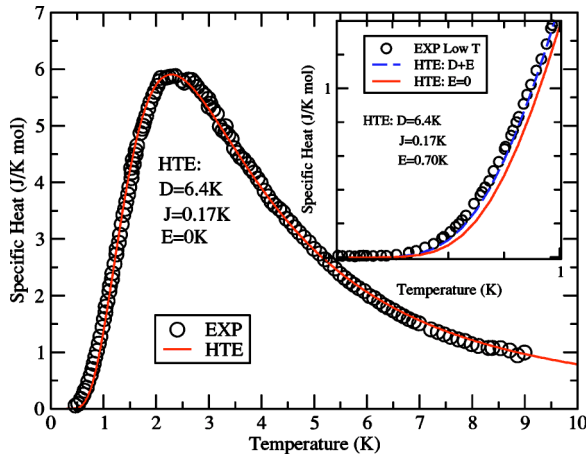
FIG. 2. (Color online) Comparison between theory and experiment (Ref. 10) for the magnetic specific heat versus temperature of the compound NENC. The conversion constant is $C_{HTE} \approx 8C_{exp}$(J/mol K). The solid line denotes the specific heat evaluated directly from the free energy (6) with the parameters $J = 0.17$ K, $D = 6.4$ K, $g = 2.24$, and $\mu_B = 0.672$ K/T. The inset shows the low temperature specific heat. Clearly the inclusion of in-plane rhombic anisotropy $E = 0.7$ K (dashed line) gives a better fit than without rhombic anisotropy (solid line).

coeffcents are not just constants, but functions of the external model parameters, e.g., the magnetic field and the coupling strength.

III. SPIN-1 COMPOUNDS

A. The compound NENC

It is known that antiferromagnetic spin-1 chains[6,7] with weak planar anisotropy can exhibit a nonmagnetic gapped phase. The large D gapped phase has been observed in the compounds NENC, NDPK, and NBYC.[10,12] In these compounds the in-plane anisotropy $x^2 - y^2$ breaks the z^2 symmetry and weakens the planar anisotropy. From experimental analysis, it was inferred that the in-plane anisotropy E in NENC[10] is negligible in comparison with the large D single-ion anisotropy, where the Nickel(II) z^2 orbit along the c-axis forms a strong crystalline field. As a result the low temperature physics is dominated by this strong crystalline field. The antiferromagnetic exchange interaction further lowers the energy but its contribution to the ground state as well as the low-lying excitations is minimal. As a consequence, the Hamiltonian (1) can be expected to describe this compound quite well. Experimentally, the specific heat was measured up to a temperature around 10 K in the absence of magnetic field.[10] A typical round peak for short range ordering at $T \approx 2.4$ K is observed, see Fig. 2. An exponential decay is detected for temperatures below approx 2.4 K. Our calculated HTE specific heat for the Hamiltonian (1) with best visual fit constants $J = 0.17$ K and $D = 6.4$ K in the case (5) (the solid line in Fig. 2) is in excellent agreement with the experimental curve in the temperature region $T > 0.8$ K. In particular, the analytic result for the specific heat gives a better fit with experimental data than the result from pertur-
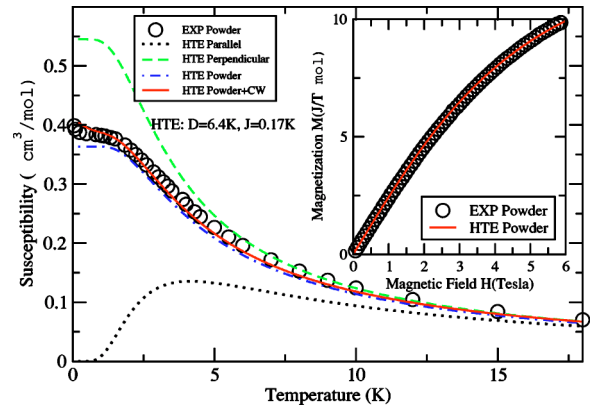

FIG. 3. (Color online) Comparison between theory and experiment (Ref. 11) for the susceptibility versus temperature of the compound NENC at $H = 0.1$ mT. The fitting curve (solid line) is obtained via the empirical relation $\chi_{powder} \approx 1/3\chi_{\parallel} + 2/3\chi_{\perp}$ together with a Curie-Weiss (CW) contribution. The inset shows the comparison between theory and experiment (Ref. 10) for the magnetization versus magnetic field of NENC at the temperature $T = 4.27$ K. A good fit for both the susceptibility and magnetization suggests the coupling constants $J = 0.17$ K, $D = 6.4$ K, $g_{\perp} = 2.18$, and $g_{\parallel} = 2.24$. The conversion constants are $\chi_{HTE} \approx 0.8123\chi_{exp}$(cgs/mol) and $M_{HTE} \approx 8.5M_{exp}$ (10^3 cgs/mol).

bation theory.[10] For low temperatures (below 0.8 K), paramagnetic impurities and a small rhombic distortion are the main reasons for the discrepancy. The inset of Fig. 2 shows that the inclusion of a small rhombic anisotropy $E = 0.7$ K gives a better fit for low temperatures than with $E = 0$. However, at high temperature this rhombic anisotropy is negligible.

As far as we know, the susceptibility was measured only for powdered samples of this compound. Moreover, the experimental susceptibility of NENC was studied only in the temperature range 50 mK–18 K under a static magnetic field $H = 0.1$ mT. From the data shown in Ref. 10 we cannot accurately estimate the contributions for the Curie-Weiss term and the paramagnetic impurity. In Fig. 3 we present our theoretical curves for the susceptibility with parallel and perpendicular field evaluated from the free energy associated with different chemical potentials. A susceptibility estimation for powdered samples using $\chi_{Powder} \approx 1/3\chi_{\parallel} + 2/3\chi_{\perp}$[16] does not fit the experimental data very well at low temperatures due to the Curie-Weiss contribution and paramagnetic impurities. A visual fit with the experimental susceptibility suggests that the contribution from the Curie-Weiss term is not negligible. We find that our theoretical susceptibility χ_{Powder} for powder with a Curie-Weiss contribution $c/(T - \theta)$ gives a satisfactory agreement with the experimental curves, where $c \approx 0.045$ cm^3 K/mol and $\theta \approx -0.9$ K. This fit suggests the values $J = 0.17$ K and $D = 6.4$ K, with $g_{\perp} = 2.18$ and $g_{\parallel} = 2.24$. From the TBA analysis we find an energy gap $\Delta \approx 5.72$ K with a parallel external magnetic field at zero temperature for these coupling constants. The typical antiferromagnetic behavior of the susceptibility with a magnetic parallel field to the axis of quantization follows from our results. This is in accordance with the behavior of the specific heat given in Fig. 2. The inset of Fig. 3 shows the
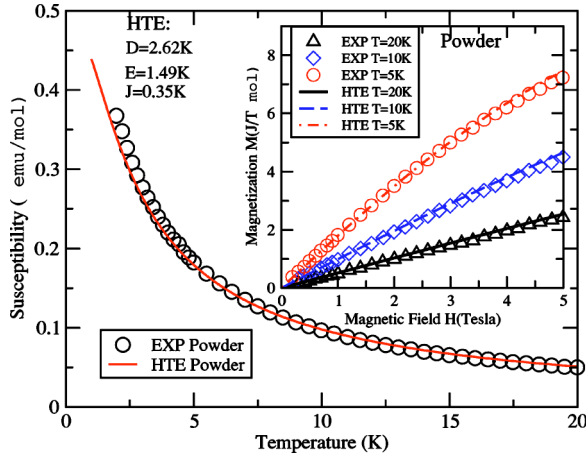
FIG. 4. (Color online) Comparison between theory and experiment (Ref. 12) for the susceptibility versus temperature of the compound NBYC. The conversion constants are the same as for NENC. The solid line is the susceptibility for the powdered samples with coupling constants $D=2.62$ K, $E=1.49$ K, and $J=0.35$ K, with $g_\parallel =g_\perp =2.05$. The small discrepancy at low temperature might be attributed to a Curie-Weiss contribution. The inset shows the magnetizations for powdered samples at 5 K, 10 K, and 20 K. In each case the theoretical results verify the existence of weak exchange coupling and in-plane rhombic anisotropy, with a strong single-ion anisotropy.

magnetization of a powdered sample at $T=4.27$ K. It is obvious that the singlet is suppressed by the temperature. Fitting suggests the empirical relation $M_{\text{Powder}}\approx 1/3M_\parallel +2/3M_\perp$ for the powdered magnetization with the same constants as before. Here $M_\parallel$ and $M_\perp$ denote the magnetization with the field parallel and perpendicular to the axis of quantization.

B. The compound NBYC

We now turn to the properties of the compound NBYC, which has also been experimentally investigated.[12] In particular, in-plane anisotropy E and a large anisotropy D are present, suggesting that the model Hamiltonian (1) may again be a good microscopic model for this type of compound. Theoretical studies based on strong-coupling expansion methods[30] suggest that the anisotropy of this compound might lie in the vicinity of the boundary between the Haldane and field-induced gapped phases.[12] However, due to the validity of the strong-coupling expansion method, the fits for specific heat, susceptibility and magnetization become increasingly inconsistent with each other as the rhombic anisotropy increases. Figure 4 presents the susceptibility for this compound. The theoretical susceptibility curve for the powdered sample is evaluated from the free energy (6) with parallel and perpendicular fields [see Eq. (12)] via the empirical formula $\chi_{\text{Powder}}\approx 1/3\chi_\parallel +2/3\chi_\perp$. A good fit for the susceptibility suggests the values $D=2.62$ K, $E=1.49$ K, $J=0.35$ K, with $g_\parallel =g_\perp =2.05$. A small discrepancy at low temperature can be attributed to a Curie-Weiss contribution term. From the TBA analysis we conclude that the ground state is gapless.
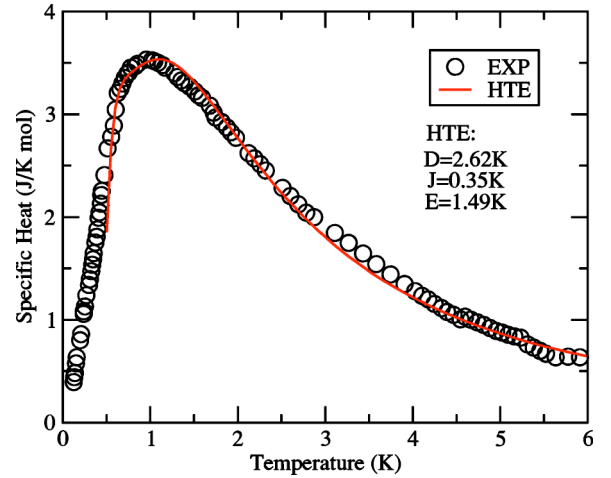

FIG. 5. (Color online) Comparison between theory and experiment (Ref. 12) for the magnetic specific heat versus temperature of the compound NBYC. The conversion constant is $C_{\text{HTE}} \approx 10C_{\text{exp}}$(J/mol K). The solid line denotes the specific heat at $H =0.1$ mT evaluated directly from the free energy (6) with the same parameters as in Fig. 4.

The inset of Fig. 4 shows the magnetization for powdered samples at 5 K, 10 K, and 20 K. Again our theoretical curves are evaluated using the empirical relation $M_{\text{Powder}} \approx 1/3M_\parallel +2/3M_\perp$ for the powdered magnetization. An overall agreement in magnetization for different temperatures gives a consistent parameter setting for the susceptibility. The singlet state is now supressed by the in-plane rhombic anisotropy and the temperature.

The specific heat was measured up to a temperature of 6 K in absence of magnetic field.[12] The theoretical specific heat evaluated from the model Hamiltonian (1) (the solid line in Fig. 5), with the same parameters used before, is in good agreement with the experimental curve in the temperature region 0.5 K to 6 K. For temperatures below 0.5 K the high temperature expansion does not converge and thus cannot provide valid predictions.
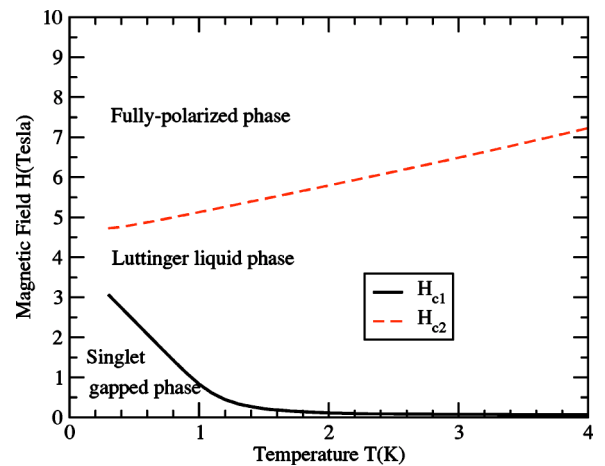

FIG. 6. (Color online) Phase diagram for the compound NENC with parameters $J=0.17$ K, $D=6.4$ K, $g=2.24$, and $\mu_B =0.672$ K/T.

IV. CONCLUSION

We have investigated the thermal and magnetic properties of spin-1 compounds with large single-ion anisotropy, such as NENC and NYBC, via the thermodynamic Bethe ansatz and the high temperature expansion for the integrable model (1). Excellent agreement was found with the experimental magnetic properties of these compounds.[31] The large single-ion anisotropy results in a nondegenerate singlet ground state which is different from the valence bond solid Haldane phase. The in-plane anisotropy weakens the energy gap.

Finally, we give the full phase diagram of the compound NENC in Fig. 6. We see that the gapped phase is quickly exhausted as the temperature increases. The magnetic ordered Luttinger liquid phase lies between the curves defined by H_{c1} and H_{c2}. The ferromagnetic polarized phase is above the H_{c2} curve. The intersection of the critical curves and the H axis indicates the estimated values $H_{c1} \approx 3.8$ T and $H_{c2} \approx 4.7$ T, which coincide with the TBA results at $T=0$ K discussed in Sec. II A. However, for the case where the in-plane anisotropy $E \neq 0$, the critical behavior is different from the phase diagram of Fig. 6. In this case the fully-polarized phase appears for $H \gg H_{c2}$ because the in-plane anisotropy mixes the doublet components $|S^z = \pm 1\rangle$. We anticipate that the exact results for the susceptibility and the magnetization of the powdered samples as well as for the compounds with parallel and perpendicular magnetic fields may find widespread use in the study of their magnetic properties and for identifying the quantum effects resulting from single-ion anisotropy. Our analytic approach via the Hamiltonian (1) may thus describe the thermal and magnetic properties of other compounds, such as NDPK,[10,11] $NiSnCl_6 \cdot 6H_2O$,[13] $[Ni(C_5H_5NO)_6](ClO_4)_2$,[14] and $Ni(NO_3)_2 \cdot 6H_2O$.[15]

[1] F. D. M. Haldane, Phys. Lett. **93A**, 464 (1983); Phys. Rev. Lett. **50**, 1153 (1983).

[2] I. Affleck, Phys. Rev. Lett. **62**, 474 (1989); I. Affleck, T. Kennedy, E. H. Lieb, and H. Tasaki, *ibid.* **59**, 799 (1987).

[3] E. Dagotto, Rep. Prog. Phys. **62**, 1525 (1999).

[4] K. Kodama, M. Takigawa, M. Horvatic, C. Berthier, H. Kageyama, Y. Ueda, S. Miyahara, F. Becca, and F. Mila, Science **298**, 395 (2002).

[5] M. Hase, I. Terasaki, and K. Uchinokura, Phys. Rev. Lett. **70**, 3651 (1993).

[6] Z. Honda, H. Asakawa, and K. Katsumata, Phys. Rev. Lett. **81**, 2566 (1998); Z. Honda, K. Katsumata, Y. Nishiyama, and I. Harada, Phys. Rev. B **63**, 064420 (2001).

[7] K. Katsumata, H. Hori, T. Takeuchi, M. Date, A. Yamagishi, and J. P. Renard, Phys. Rev. Lett. **63**, 86 (1989).

[8] M. Oshikawa, M. Yamanaka, and I. Affleck, Phys. Rev. Lett. **78**, 1984 (1997).

[9] A. M. Tsvelik, Phys. Rev. B **42**, 10 499 (1990).

[10] A. Feher, M. Orendáč, A. Orendáčová, and E. Čižmár, Low Temp. Phys. **28**, 551 (2002); M. Orendáč *et al.*, Phys. Rev. B **52**, 3435 (1995).

[11] M. Orendáč, A. Orendáčová, A. Feher, J. Chomac, S. A. Zvyagin, V. V. Eremenko, and V. V. Pishko, J. Magn. Magn. Mater. **140–144**, 1643 (1995).

[12] M. Orendáč, E. Čižmár, A. Orendáčová, J. Cernak, A. Feher, M. W. Meisel, K. A. Abboud, S. Zvyagin, M. Sieling, T. Reith, and B. Luthi, Phys. Rev. B **61**, 3223 (2000).

[13] B. E. Myers, L. G. Polgar, and S. A. Friedberg, Phys. Rev. B **6**, 3488 (1972).

[14] R. L. Carlin, C. J. O'Connor, and S. N. Bhatia, J. Am. Chem. Soc. **98**, 3523 (1976).

[15] A. Herweijer and S. A. Friedberg, Phys. Rev. B **4**, 4009 (1971).

[16] R. L. Carlin, *Magnetochemistry* (Springer-Verlag, New York, 1986).

[17] M. T. Batchelor, X.-W. Guan, N. Oelkers, K. Sakai, Z. Tsuboi, and A. Foerster, Phys. Rev. Lett. **91**, 217202 (2003).

[18] M. Takahashi, Prog. Theor. Phys. **46**, 401 (1971); P. Schlottmann, Phys. Rev. B **33**, 4880 (1986).

[19] M. Shiroishi and M. Takahashi, Phys. Rev. Lett. **89**, 117201 (2002).

[20] Z. Tsuboi, J. Phys. A **36**, 1493 (2003); J. Phys. A **37**, 1747 (2004).

[21] J. L. Gavilano, S. Mushkolaj, H. R. Ott, P. Millet, and F. Mila, Phys. Rev. Lett. **85**, 409 (2000); P. Millet *et al.*,*ibid.* **83**, 4176 (1999).

[22] G. V. Uimin, JETP Lett. **12**, 225 (1970).

[23] B. Sutherland, Phys. Rev. B **12**, 3795 (1975).

[24] A. Fujii and A. Klümper, Nucl. Phys. B **546**, 751 (1999).

[25] M. T. Batchelor, J. de Gier, and M. Maslen, J. Stat. Phys. **102**, 559 (2001).

[26] M. T. Batchelor, X.-W. Guan, A. Foerster, and H.-Q. Zhou, New J. Phys. **5**, 107 (2003); M. T. Batchelor, X.-W. Guan, N. Oelkers, and Z.-J. Ying, J. Stat. Phys. **116**, 571 (2004).

[27] Z.-J. Ying, A. Foerster, X.-W. Guan, B. Chen, and I. Roditi, Eur. Phys. J. B **38**, 535 (2004); Z.-J. Ying, I. Roditi, A. Foerster, and B. Chen, cond-mat/0403520.

[28] M. Suzuki, Phys. Rev. B **31**, 2957 (1985); A. Klümper, Ann. Phys. (Leipzig) **1**, 540 (1992).

[29] Equivalently, we can consider the external field parallel to the z axis, whereas the crystalline field and orbital splitting are along x or y axis.

[30] N. Papanicolaou and P. N. Spathis, Phys. Rev. B **52**, 16 001 (1995).

[31] We find similar agreement for the compound NDPK.